Water Air Soil Pollut (2020) 231: 187
https://doi.org/10.1007/s11270-020-04518-w

Preparation of Sewage Sludge–Based Activated Carbon for Hydrogen Sulphide Removal

M. J. Luján-Facundo · M. I. Iborra-Clar · J. A. Mendoza-Roca · M. I. Alcaina-Miranda · A. M. Maciá · C. Lardín · L. Pastor · J. Claros

Received: 23 December 2019 / Accepted: 5 March 2020 / Published online: 16 April 2020
© Springer Nature Switzerland AG 2020

Abstract The circular economy concept boosts the use of wastes as secondary raw materials in the EU renewable and sustainable framework. In wastewater treatment plants (WWTP), sludge is one of the most important wastes, and its management is being widely discussed in the last years. In this work, sewage sludge from WWTP was employed as raw material for producing activated carbon (AC) by physical-chemical activation. The prepared AC was subsequently tested for hydrogen sulphide removal in view of its further use in deodorization in a WWTP. The effects of the activation temperature and the chemical agent used (NaOH and KOH) during the activation process were studied. On the one hand, the characteristics of each AC fabricated were analysed in terms of BET (Brunauer-Emmett-Teller) surface area, pore and micropore volume, pore diameter, surface morphology and zeta potential. On the other hand, BET isotherms were also calculated. Finally, both the prepared AC and a commercial AC were tested for H_2S removal from a gas stream. Results demonstrated that the optimum physical and chemical activation temperature was 600 °C and 1000 °C, respectively, and the best activated agent tested was KOH. The prepared AC showed excellent properties (specific surface area around 300 m^2/g) for H_2S removal, even better efficiencies than those achieved by the tested commercial AC.

Keywords Activated carbon · Adsorption · Deodorization · Wastewater sludge

M. J. Luján-Facundo (✉) · M. I. Iborra-Clar · J. A. Mendoza-Roca · M. I. Alcaina-Miranda
Instituto de Seguridad Industrial, Radiofísica y Medioambiental, Universitat Politècnica de València, Camino de Vera, s/n, 46022 Valencia, Valencia, Spain
e-mail: malufa@etsii.upv.es

A. M. Maciá
Molina del Segura WWTP. UTE Molina del Segura – Alguazas, Campotéjar Baja, s/n bajo, 30500 Molina del Segura, Murcia, Spain

C. Lardín
Regional Entity for Sanitation and Wastewater Treatment in Murcia, Spain (ESAMUR), Complejo Espinardo CN-301, Calle Santiago Navarro, 4, 30100 Espinardo, Murcia, Spain

L. Pastor · J. Claros
Depuración de Aguas del Mediterráneo (DAM), Avenida Benjamín Franklin, 21, Parque Tecnológico, 46980 Paterna, Valencia, Spain

1 Introduction

In the last years, the emerging concept of circular economy is changing the mission of wastewater treatment plants. The main goal of these plants is no longer to discharge the treated effluent meeting the legal standards but to recover energy and materials from the wastewater. In this way, nutrient recovery (Peng et al. 2018; Ye et al. 2018), optimization of energy recovery from anaerobic processes (Kimura et al. 2017) and sludge valorization are topics of increasing interest.

Sludge management is a non-solved issue. The reuse of wastewater sludge for agricultural purposes is threatened by the presence of persistent organic compounds and pathogens, and some countries have restricted the

use of wastewater sludge in the agriculture (G. Mininni et al. 2015).

One of the applications studied for the wastewater sludge in recent years has been its use for making activated carbon. The interest for the preparation of activated carbon from organic wastes increased in the last decade of the twentieth century as reported by Dias et al. (2007). These authors summarized the wastes used for the activated carbon preparation and the applications of the prepared carbons. In this way, cherry stones, corn cobs, olive pits, walnut shells and other wastes have been employed for this purpose. Chiavola (2013) reviewed the main findings about the valorization of organic wastes as activated carbon. This author summarizes the use of activated carbon prepared from peanut shells, olive stone and apricot stone of different works.

The aforementioned trend to circular economy implies that valorization of organic wastes as activated carbon is still a current goal especially when high amounts of organic wastes are available. As an example, Pandiarajan et al. (2018) prepared activated carbon from orange peel to separate herbicides. Activation was carried out using KOH in the ratio 1:2 and reaching temperatures of 700 °C. Other examples are works in which authors have used coconut (Andrade et al. 2018) and corncob (Zhu et al. 2018).

Focusing on wastewater sludge, it has to be highlighted that sludge is theoretically an appropriate source for activated carbon due to great availability and high organic matter content. Li et al. (2011) and Wang et al. (2008) prepared activated carbon from activated sludge from a municipal wastewater treatment plant and from sludge from a paper mill wastewater treatment plant, respectively. In both cases, the prepared activated carbon was used for dye removal. More recently, Qiu and Huang (2015) made activated carbon from sewage sludge using $ZnCl_2$ for the activation with the aim of separating two commercial dyes from wastewater. Other applications of sludge-based activated carbons are the separation of heavy metals (Li et al. 2018) and pharmaceutical compounds (dos Reis et al. 2016).

Concerning the preparation processes, Hadi et al. (2015) concluded in a review article that chemical activation yielded considerable higher specific surface areas than physical activation procedures. In this way, it is very important to focus on chemical activation.

In this work, chemically activated carbon from sewage sludge has been prepared for hydrogen sulphide adsorption. Until now, there are limited papers dealing with this topic. Only Li et al. (2015) aimed at this application. However, it would be of great importance to use the sludge in the same wastewater treatment plant for odour elimination, for example in the final step of thickeners or in the sludge dehydration. In addition, preparation of the activated carbon in the same plant would avoid transport costs. This fact together with the uncertainty about the future sludge management alternatives make that the preparation of activated carbon for hydrogen sulphide removal may have a promising future.

2 Materials and Methods

2.1 Sludge Characterization

Sludge from municipal WWTP located in Murcia Region (Spain) was used for activated carbon preparation. The characterization of the sludge included the measurement of pH, conductivity, total suspended solids (TSS), volatile suspended solids (VSS), total COD (chemical oxygen demand) and ammonium nitrogen (NH_4-N). In addition, sludge was also pre-treated in order to measure the following parameters in the soluble fraction: soluble COD, total nitrogen (TN), nitrates (NO_3-N), total phosphorous (TP), calcium (Ca^{+2}) and magnesium (Mg^{+2}). The pre-treatment consisted in centrifuging at 10.000 rpm for 15 min and filtering the clarified water for the analysis.

pH and conductivity measurements were carried out with pHMeter GLP 21^+ and EC-Meter GLP 31^+ (CRISON), respectively. TSS and VSS were measured according to Standard Methods (APHA, AWWA, WEF, 2005). COD, TN, NO_3-N, TP, Ca^{+2} and Mg^{+2} were analysed using kits from Merck (Spain). NH^4-N content was determined using a "Pro-Nitro M" distiller (P-Selecta, Spain).

The properties of the analysed sludge are in Table 1. It can be observed that all the parameters are in the range for sludge characterization (Ping et al., 2020). In addition, the high COD content is especially favourable for activated carbon preparation (Li et al. 2020).

2.2 Activated Carbon Preparation

Two series of experiments were performed in the AC preparation. In the first one, NaOH and KOH

Table 1 Sludge characterization for activated carbon preparation

Parameter	Value
TN (mg/L)	1370
NO_3-N (mg/L)	8.84
PT (mg/L)	51.30
Total COD (mg/L)	7683
Soluble COD (mg/L)	1569
Ca^{+2} (mg/L)	180.30
Mg^{+2} (mg/L)	60
NH_4-N (mg/L)	949.45
pH	7.80
Conductivity (mS/cm)	16.71
TSS (g/L)	7.55
VSS (g/L)	4

(from Panreac) were used as activating agents. Table 2 summarizes the experimental values of the variables used during the first set of experiments. The physical activation is a pyrolysis process, and the chemical activation was carried out by mixing the sludge with the activated agent. The heat treatment of the samples was conducted in a furnace from Nabertherm model RSRB 120/750/11. Pure nitrogen gas was used to produce an inert gas atmosphere. The flow rate of nitrogen was 300 mL/min, and samples were heated up to the previously programmed temperature at a heating rate of 20 °C/min.

From the first set of experiments, the optimal experimental conditions were chosen: physical activation temperature of 600 °C, chemical activation temperature of 1000 °C and KOH as activated agent. At these experimental conditions, the second series of experiments was performed (Table 3). It was decided to include also $ZnCl_2$ as activated agent in order to take into account results from previous publications (Rawal et al., 2018; Tian et al., 2019).

2.3 Commercial Activated Carbon

In order to compare the effectiveness of the prepared AC, a commercial granular AC for gas adsorption was tested in this study. This AC is from VWR (reference number 22631.293). Table 4 illustrates the main characteristics given by the supplier.

2.4 Characterization of Prepared Activated Carbon

2.4.1 Specific Surface Area and Isotherm Analysis

The prepared activated carbon was characterized in terms of surface area (S_{BET}), total pore volume (V_t) and average pore diameter (d_a). BET method was applied using a multi-port surface area and porosimetry analyser ASAP 2420 from Micromeritics (USA). Using this technology, the micropore volume (V_m) was also calculated. Total pore volume was calculated from the amount of adsorbed N_2 at relative pressure (P/P_0) of 0.99, and average pore diameter was calculated following Eq. 1 as previously published in several studies (Pezoti et al. 2016; Zhang et al. 2019):

$$d_a = \frac{4000 \cdot V_t}{S_{BET}} \quad (1)$$

In addition, adsorption isotherms were obtained using the prepared AC as shown in Tables 2 and 3.

Table 2 Data for the activated carbon preparation in the first set of experiments

Physical activation (°C)	Chemical activation (°C)	Activating agent	Reference
600	1000	NaOH	A1
600	1000	KOH	A2
800	1000	NaOH	A3
800	1000	KOH	A4
1000	600	NaOH	A5
1000	600	KOH	A6
1000	800	NaOH	A7
1000	800	KOH	A8

Table 3 Data for the activated carbon preparation in the second set of experiments

Activating agent	Activating agent/sludge ratio (mL/g)	Reference
KOH	0.3	B1
KOH	0.4	B2
KOH	0.5	B3
KOH	0.7	B4
$ZnCl_2$	0.3	B5
$ZnCl_2$	0.4	B6
$ZnCl_2$	0.5	B7
$ZnCl_2$	0.7	B8

Adsorption isotherm analysis is very important to study the interaction between the adsorbate and the adsorbent of a system (Cheng et al. 2018). In this study, BET isotherms were calculated. BET model assumes that adsorption process occurs in a multilayer of adsorbates with lateral interactions (Carrete et al. 2011).

The mathematical expression BET isotherm is described in Eq. 2:

$$\frac{P}{V\cdot(P_0-P)}=\frac{1}{V_m\cdot c}+\frac{c-1}{V_m\cdot c}\cdot\frac{P}{P_0} \quad (2)$$

where P (mm Hg) and P_0 (mm Hg) are the equilibrium and the saturation pressures, respectively, of adsorbates at the adsorption temperature, V (cm^3/g) and V_m (cm^3/g) are the adsorbed gas quantity and the monolayer adsorbed gas quantity, respectively, and c is the BET constant.

2.4.2 Microscopy Analysis

The surface morphologies of the prepared AC were examined by observation of the microporous structure by means of a Field Emission Scanning Microscopy (FE-SEM) model Ultra 55 from Oxford Instruments (UK).

Table 4 Technical characteristics of the commercial AC

Parameter	Values
Density (g/cm^3)	2
Molecular weight (g/mol)	12.01
Melting point (°C)	3550
Benzene adsorption (%)	38–42

2.4.3 Zeta Potential

Zeta potential of the prepared AC was measured by Zetasizer Nano ZS90 (Malvern instruments, Malvern, UK). Zeta potential of the AC was measured by mixing the AC with distilled water at pH 7.5.

2.5 Activated Carbon Regeneration Procedure

A regeneration process was carried out for the prepared activated carbon. The spent AC was placed in a laboratory beaker with 500 mL of NaOH at pH 10. This solution was stirred in a temperature controlled shaker at 200 rpm and 90 °C during 2 h. After this chemical regeneration process, the AC was filtered (with a paper filter of 60 μm) and rinsed with water until a neutral pH was reached. Afterwards, the AC was filtered again and was dried at 105 °C during 12 h.

2.6 Hydrogen Sulphide Adsorption Equipment

Tests with laboratory columns were used for gas adsorption with the selected AC. Gas cylinders (provided by Abelló-Linde, Spain) containing a mixture of H_2S/N_2 with a H_2S concentration of 80 mg/L provided the feed to the adsorption column. These experiments were carried out in a glass column of 1.5 cm internal diameter and 20 cm length. A felt layer and a circular mesh were placed at the bottom of the column to ensure the correct package of the activated carbon. Figure 1 shows the experimental set up used for the experiments.

Bed heights of the packed AC, mass of the AC and feed gas flow rate used in the tests are summarized in Table 5. The tests were stopped when the outlet and inlet H_2S concentrations were approximately the same. It is important to mention that only the prepared ACs under the selected conditions was tested in the adsorption column.

In addition, in order to compare the saturation capacity of each AC tested, it was calculated the amount of H_2S adsorbed per gram of AC used as it was expressed in Eq. 3. This equation was previously applied also employed by Kuroda et al. (2018).

$$\text{Capacity (mg H2S adsorbed/g AC used)}=\frac{\left[C_f\cdot t_f-\int_0^{t_f}C(t)dt\right]\cdot\frac{34g}{mol}\cdot Q}{m_{AC}\cdot 22,4\ L/mol} \quad (3)$$

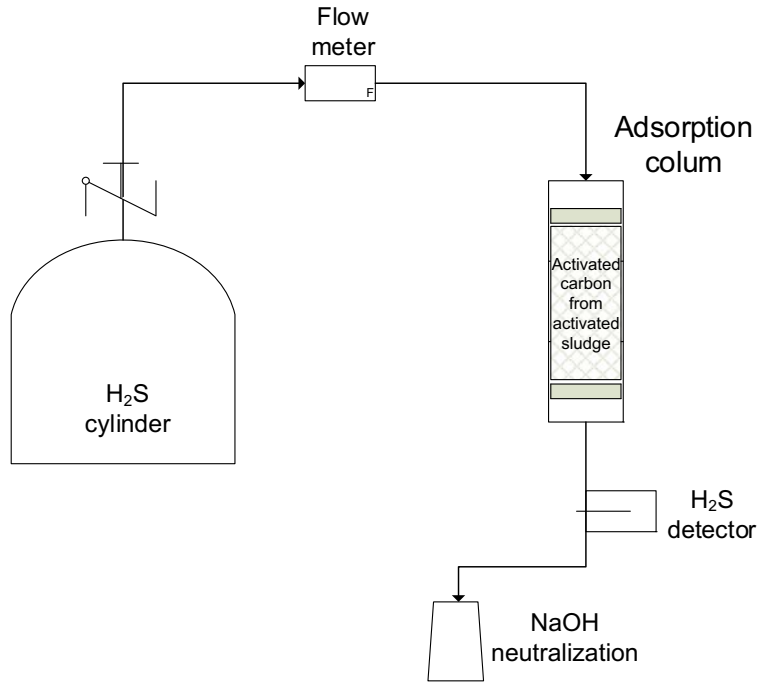

Fig. 1 Experimental set up used for the adsorption column experiments

where C_f and t_f are the final H_2S concentration and time detected, respectively, Q is the flow rate employed and m_{AC} is the AC mass used for each experiment.

3 Results and Discussion

3.1 Prepared Activated Carbon Characteristics

3.1.1 Effect of Temperature and Activating Agent

Pyrolysis temperature, carbonization time and impregnation ratio are the main parameters that can influence the surface area of the made ACs (Kacan, 2016). In order to study the effect of temperature, Table 6 illustrates the Brunauer-Emmet-Teller surface area (S_{BET}), the total pore volume (V_t), the micropore volume (V_m) and the average pore diameter (d_a) of the different samples of activated carbons that were obtained by means of the analysis of N_2 adsorption. These results indicated that there was no direct influence of the physical activation temperature on the S_{BET}, V_t and V_m since the highest results were achieved for the lowest temperatures tested. The same conclusion was reported by Wang et al. (2018) who stated that a pyrolysis temperature of 600° was sufficient for sludge carbonization. However, it can be observed that when chemical activation temperature increased, the $S_{BET,}$ V_t and V_m increased. In addition, the best activating agent was KOH, also in terms of $S_{BET,}$ V_t and $V_{m.}$ Concerning the average pore diameter, all the values ranged between 2 and 20 nm, which means that no significant differences among the prepared ACs were found. The average pore diameter depends mainly on the reaction time, which was maintained constant in all the tests. Temperature also influences the pore size. However, the relation

Table 5 Experimental variables applied for the adsorption experiments

Test number	AC type	AC mass (g)	Bed heights (cm)	Flow rate (L/h)
1	Commercial AC	10.21	4	43
2	Prepared AC 1	2.09	2	43
3	Prepared AC 2	3.51	2	43
4	Regenerated AC 2	2.04	2	43

Table 6 Surface area (S_{BET}), total pore volume (V_t), micropore volume (V_m) and average pore diameter (d_a) of the first set of experiments

Activated carbon type	A1	A2	A3	A4	A5	A6	A7	A8
S_{BET} (m^2/g)	140.29 ± 7.01	375.13 ± 18.75	185.95 ± 9.29	236.4 ± 11.82	143.3 ± 7.17	1.57 ± 0.08	55.57 ± 2.78	187.34 ± 9.37
V_m (cm^3/g)	0.0488 ± 0.05	0.1587 ± 0	0.0617 ± 0	0.1031 ± 0.01	0.0468 ± 0	0.002 ± 0	0.012 ± 0	0.0595 ± 0
Vt (cm^3/g)	0.1765 ± 0.17	0.3152 ± 0.01	0.2321 ± 0.01	0.1465 ± 0.01	0.1148 ± 0	0.0072 ± 0	0.1594 ± 0.01	0.1917 ± 0.01
d_a (nm)	5.03 ± 5.03	3.36 ± 0.17	4.99 ± 0.25	2.48 ± 0.12	3.2 ± 0.16	18.32 ± 0.91	11.48 ± 0.57	4.09 ± 0.20

between temperature and pore size is complex. In this way, Satya Sai and Krishnaiah (2005) reported that at 800 °C, low size pores are formed, but at 850 °C, the smaller pores become larger by coalescence phenomena. It explains that no relation between the experimental conditions and the average pore diameter was found. Taking into account these results, the best AC was the AC *A2* since it was made with the highest S_{BET}, V_t and $V_{m.}$

These results are in concordance with other studies found in the literature of AC preparation from sewage sludge. For example, Li et al. (2011) fabricated AC from sludge and achieved an AC with specific surface area between 130 and 140 m^2/g. Wang et al. (2018) obtained an AC from sludge with a higher surface area (641.56 m^2/g).

Regarding AC preparation from other raw materials, Li et al. (2019) reported that AC preparation from petroleum coke by KOH activation achieved S_{BET} between 892 and 1763 m^2/g and V_t values between 0.39 and 0.48 cm^3/g. Kazak et al. (2018) published that AC preparation from molasses-to-ethanol-process waste by KOH activation presented a S_{BET} area of 1042 m^2/g and V_t of 0.691 cm^3/g. Sulaiman et al. (2018) fabricated AC from cassava stem, and the carbon fabricated showed a maximum S_{BET} area of 653.93 m^2/g. The difference between the previously published results and those reported in this study in terms of surface area was due to the raw material employed. Sewage sludge is not the best option to produce AC, but results presented here demonstrated that it is a waste whose activation can produce an adsorbent with a S_{BET} high enough to be competitive compared with other activated carbon materials (Chen et al. 2019).

3.1.2 Comparison of KOH and $ZnCl_2$ as Activating Agents

According to Tian et al. (2019), H_3PO_4, KOH and $ZnCl_2$ are common activating agents in the AC preparation. In order to study the $ZnCl_2$ effect on the AC characteristics (Table 7), the experimental conditions from the first set of experiments (physical temperature of 600 °C, chemical temperature of 1000 °C and KOH as activated agent, AC type *A2*) study the effect of $ZnCl_2$ in comparison with KOH as activating agent. It is observed in Table 7 that using KOH as activating agent (AC *B1*, *B2*, *B3* and *B4*) led to higher S_{BET} and V_t than those obtained by using $ZnCl_2$ (AC *B5*, *B6*, *B7* and *B8*). These results

Table 7 Surface area (S_{BET}), total pore volume (V_t), micropore volume (V_m) and average pore diameter (d_a) of the second set of experiments

Activated carbon type	B1	B2	B3	B4	B5	B6	B7	B8
Activated agent	KOH	KOH	KOH	KOH	$ZnCl_2$	$ZnCl_2$	$ZnCl_2$	$ZnCl_2$
S_{BET} (m^2/g)	287.99 ± 14.40	338.54 ± 16.93	342.78 ± 17.14	340.18 ± 17.01	184.42 ± 9.22	204.95 ± 10.24	228.25 ± 11.41	228.59 ± 11.42
V_m (cm^3/g)	0.1138 ± 0.01	0.1374 ± 0.01	0.1307 ± 0.01	0.1117 ± 0.01	0.0524 ± 0	0.0621 ± 0	0.0702 ± 0	0.0698 ± 0
V_t (cm^3/g)	0.2051 ± 0.01	0.2190 ± 0.01	0.2471 ± 0.01	0.2850 ± 0.01	0.1757 ± 0.01	0.1828 ± 0.01	0.2065 ± 0.01	0.2135 ± 0.01
d_a (nm)	2.85 ± 0.14	2.59 ± 0.13	2.88 ± 0.14	3.35 ± 0.17	3.81 ± 0.19	3.57 ± 0.18	3.62 ± 0.18	3.74 ± 0.19

are interesting since KOH is less expensive toxic than $ZnCl_2$ (Arami-Niya et al. 2010; Donald et al. 2011). In addition, as it is observed in Table 7, as activation agent/sludge ratio increased, S_{BET} increased for both activating agents. These results are in the same range as those previously published by Sun et al. (2018), who prepared activated biochar from mixed waste plastic using $ZnCl_2$ as activated agent and obtained values of S_{BET} between 661 and 1032 m^2/g, V_t values between 0.44 and 0.64 cm^3/g and d_a values between 2.15 and 3.62 nm.

3.1.3 Isotherm Analysis

According to the International Union of Pure and Applied Chemistry (IUPAC) standard classification system, there are six different types of adsorption Sing et al. (1985) as it can be observed in a previous publication (Wei Yu 2018). In this way, depending of the shape of the adsorption isotherm, the properties of the adsorbate and solid adsorbent and the pore-space geometry can be different. Detailed information about it can be found in (Sing et al. 1985). Figure 2 represents BET isotherms of prepared AC in the tests *A2* and *B3*. It can be observed that both curves showed a convex curvature at low relative pressures (P/P_0 lower than 0.2) and then a slight hysteresis towards saturation. Adsorption normally occurs in a nonporous or a macroporous layer (Sing et al. 1985). In this way, adsorption process seems to be in the multi-layer coverage since there is a clear inflexion in the isotherm (Lapham and Lapham 2017).

Table 8 shows the BET c-value for all the AC fabricated. According to Ladavos et al. (2012), who investigated the BET isotherm model in porous materials for gas adsorption, c-values should be greater than zero. Lapham and Lapham (2017) published that BET c-values higher than 20 confirms that S_{BET} and adsorption isotherms previously calculated are reliable and valid. As it is observed in Table 8, c-values were always positive and higher than 20.

3.1.4 Microscopy Results

The surface morphologies of the prepared AC with the highest areas (*A2* and *B3* for the first and second series of experiments, respectively) are shown in Fig. 3. Both AC had a very similar surface area (375 and 342 m^2/g for AC of *A2* and *B3*, respectively), which is in agreement with these FE-SEM pictures since a very similar structure is observed in Fig. 3. FE-SEM images show a

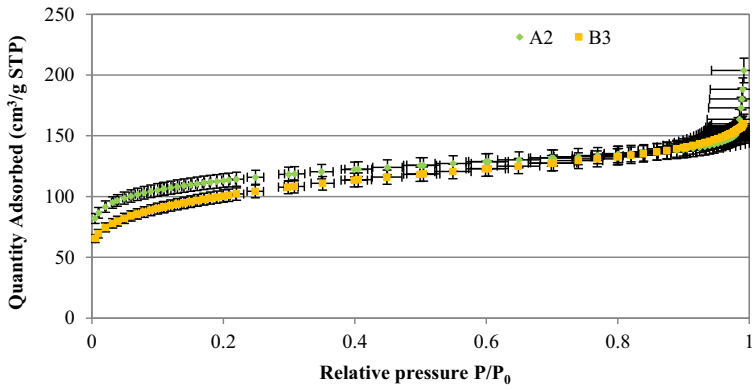

Fig. 2 BET isotherm for AC *A2* and *B3*

highly porous structure, a relatively uniform surface and without the crevices appearance. The surface seems to be heterogeneous and with a variety of randomly distributed micropores and nanopores of different sizes (diameter around 0.1 μm). The different pore sizes can be attributed to the organic matter decomposition during the carbonization process. In addition, the size and the presence of particles are reduced due to material loss during pyrolysis process.

3.1.5 Zeta Potential Results

Zeta potential of the tested AC for H_2S adsorption (*AC1* and *AC2*) was measured to study possible interactions between the AC and the H_2S during the adsorption process. The mean value of zeta potential of *AC1* and *AC2* was -24.9 ± 0.8 mV and -25.2 ± 1 mV, respectively. Thus, both values were very similar. They clearly showed the negative charge of the prepared AC. This fact suggests that positively charged pollutants will be more easily adsorbed by these AC. For H_2S adsorption, the presence of H^+ protons forming a dipole moment with S^{-2} can result favourable for the H_2S adsorption. This fact is due to the negative charge of the prepared AC and the positive electric density of the H^+. In addition, this result is in concordance with Li et al. (2011) who also published a negative zeta potential value of sludge-based AC (between -35 and -37 mV).

3.2 Hydrogen Sulphide Adsorption

In order to study the effectiveness in the H_2S removal of the prepared AC, regenerated AC and a commercial AC, breakthrough curves have been plotted (Fig. 4). H_2S retention capacity was measured using an H_2S initial concentration of 80 ppm in the feed gas. It can be observed that the breakpoint occurred at approximately 30 min for commercial AC, whereas for the AC 1, AC 2 and regenerated AC 2, it occurred at about 140, 90 and 7 min, respectively. It can be observed that the prepared ACs showed higher affinity to H_2S retention than the commercial AC since the breakpoints occurred later than in the case of the commercial AC. As expected, since no thermal treatment was performed, the regenerated AC 2 did not show the same efficiency than the new AC 2. These results are in concordance with previous studies such us Zhang et al. (2016) who prepared AC from black liquor for hydrogen sulphide removal and reported that the breakpoint was around 150 min. Regarding H_2S adsorption mechanism on activated carbon, according Shen et al. (2018), AC can facilitate the H_2S molecule dissociation and offers active sites for H_2S adsorption.

In order to compare the saturation capacity of each AC, Table 9 shows the relation between the H_2S

Table 8 BET c-value for each prepared AC

AC first set of experiments	**A1**	**A2**	**A3**	**A4**	**A5**	**A6**	**A7**	**A8**
BET c-value	335.44	302.08	291.86	179.92	339.55	29.84	1092.56	465.06
AC second set of experiments	**B1**	**B2**	**B3**	**B4**	**B5**	**B6**	**B7**	**B8**
BET c-value	243.88	467.17	241.78	233.18	431.71	442.36	300.84	364.46

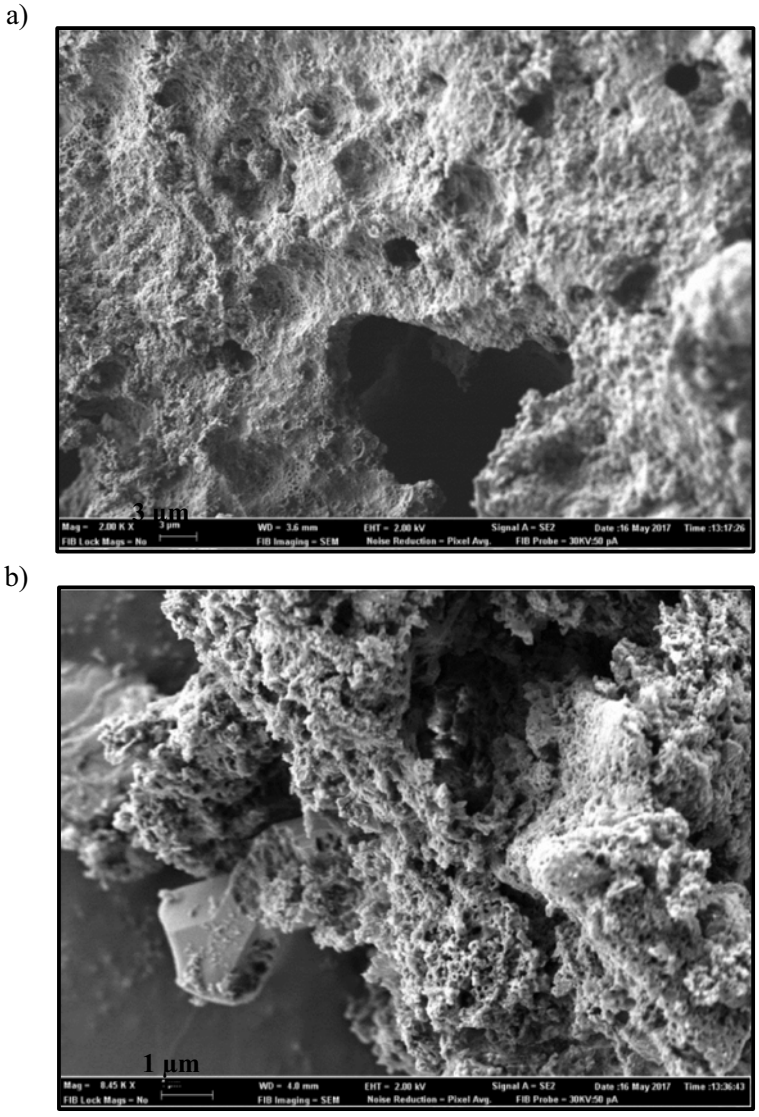

Fig. 3 FE-SEM images of the prepared AC samples number **a** *A2* and **b** *B3*

adsorbed mass (in mg) and the AC mass (in g) employed in each test. It can be observed, as commented above, that the commercial AC had a lower capacity than the prepared AC, even than the regenerated AC. De Falco et al. (2018) tested a commercial AC impregnated with Cu and Zn for H_2S removal and achieved an adsorption capacity values between 6.8 and 49.64 mg/g. However, Aslam et al. (2015) prepared AC from oil fly ash for H_2S removal from a gas stream and obtained saturation capacity values around 0.1 mg/g. Taking into account these results, it can be concluded that the results published here are in the range with previous results published in the bibliography.

4 Conclusions

In this study, AC with interesting properties for hydrogen sulphide removal was prepared from sewage sludge by physical-chemical activation. The optimum physical and chemical activation temperature was 600 °C and 1000 °C, respectively. Regarding the best activated agent, KOH achieved the most interesting results in terms of specific surface area (values around 300 and 340 m^2/g for the tested conditions). Zeta potential of the prepared AC was negative (around − 25 mV), and it was observed a heterogeneous pore size distribution in the surface morphology of the adsorbent materials. In

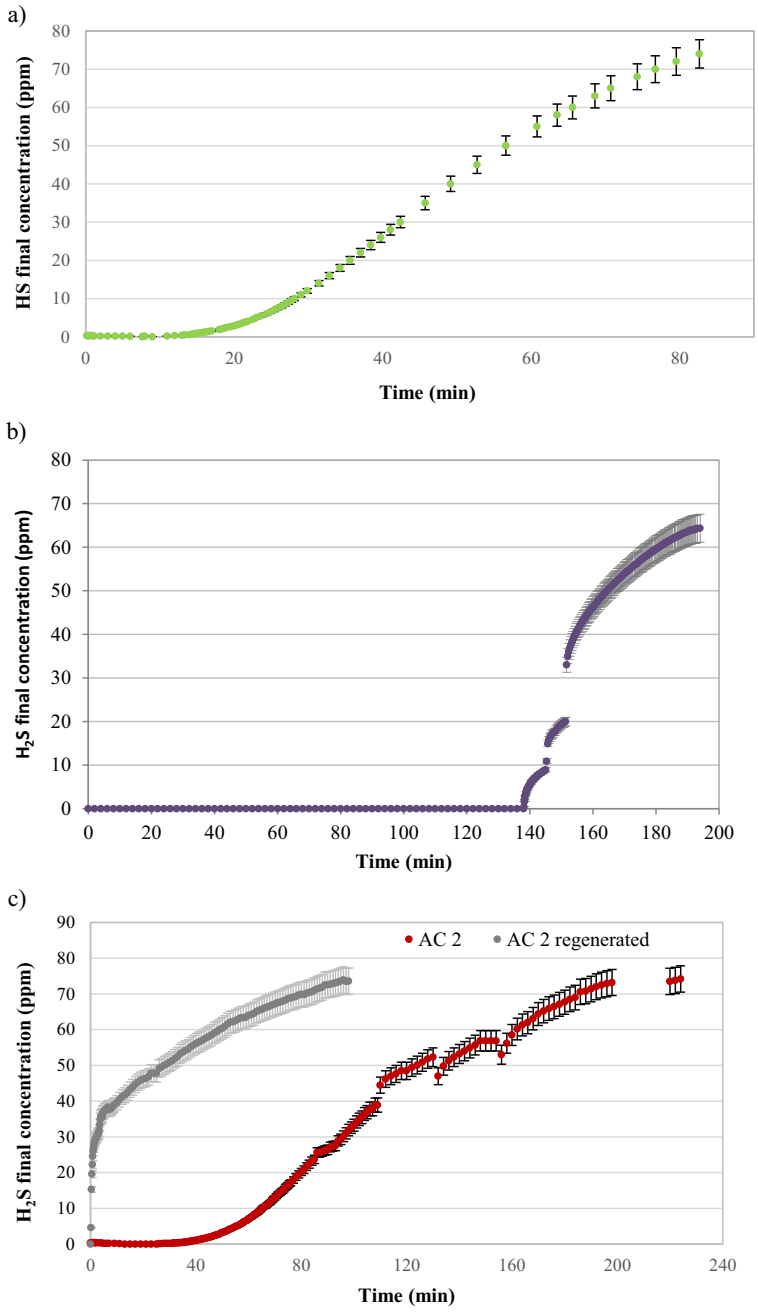

Fig. 4 Experimental and breakthrough curves for **a** commercial AC, **b** AC 1 and **c** AC 2

Table 9 Capacity of each AC

AC type	Commercial AC	AC 1	AC 2	Regenerated AC 2
Adsorbed H_2S (mg)/AC mass (g)	0.37	5.0	1.96	0.78

addition, the experimental results were adjusted to BET isotherms, which confirms that the adsorption process occurs in a multi-layer space. Finally, results from the prepared and the commercial AC tested for H_2S removal demonstrated that the prepared AC was effective, even more than the tested commercial AC, for H_2S removal. As a general conclusion, it can be confirmed that the use

of prepared AC from sewage sludge for odour removal could be of great interest in a recent future.

References

Andrade, S. N., Veloso, C. M., Fontan, R. C. I., Bonomo, R. C. F., Santos, L. S., Brito, M. J. P., & Diniz, G. A. (2018). Chemical-activated carbon from coconut (Cocos nucifera) endocarp waste and its application in the adsorption of beta lactoglobulin protein. *Revista Mexicana de Ingenieria Quimica, 17*(2), 463–475.

APHA, AWWA, WEF. (2005). Standard methods for the examination of water and wastewater. Washington.

Arami-Niya, A., Daud, W. M. A. W., & Mjalli, F. S. (2010). Using granular activated carbon prepared from oil palm shell by ZnCl 2 and physical activation for methane adsorption. *Journal of Analytical and Applied Pyrolysis, 89*, 197–203.

Aslam, Z., Shawabkeh, R., Hussein, I., Al-Baghli, N., & Eic, M. (2015). Synthesis of activated carbon from oil fly ash for removal of H2S from gas stream. *Applied Surface Science, 327*, 107–115.

Carrete, J., García, M., Rodríguez, J. R., Cabeza, O., & Varela, L. M. (2011). Theoretical model for moisture adsorption on ionic liquids: a modified Brunauer–Emmet–Teller isotherm approach. *Fluid Phase Equilibria, 301*, 118–122.

Chen, C. L., Park, S. W., Su, J. F., Yu, Y. H., Heo, J. E., Kim, K. D., & Huang, C. P. (2019). The adsorption characteristics of fluoride on commercial activated carbon treated with quaternary ammonium salts (Quats). *Science of the Total Environment, 693*, 133605.

Cheng, S., Zhang, L., Ma, A., Xia, H., Peng, J., Li, C., & Shu, J. (2018). Comparison of activated carbon and iron/cerium modified activated carbon to remove methylene blue from wastewater. *Journal of Environmental Sciences, 65*, 92–102.

Chiavola, A. (2013). Textiles. *Water Environment Research, 85*, 1581–1600.

De Falco, G., Montagnaro, F., Balsamo, M., Erto, A., Deorsola, F. A., Lisi, L., & Cimino, S. (2018). Synergic effect of Zn and Cu oxides dispersed on activated carbon during reactive adsorption of H 2 S at room temperature. *Microporous and Mesoporous Materials, 257*, 135–146.

Dias, J. M., Alvim-Ferraz, M. C. M., Almeida, M. F., Rivera-Utrilla, J., & Sánchez-Polo, M. (2007). Waste materials for activated carbon preparation and its use in aqueous-phase treatment: a review. *Journal of Environmental Management, 85*, 833–846.

Donald, J., Ohtsuka, Y., & Xu, C. C. (2011). Effects of activation agents and intrinsic minerals on pore development in activated carbons derived from a Canadian peat. *Materials Letters, 65*, 744–747.

dos Reis, G. S., Mahbub, M. K. B., Wilhelm, M., Lima, E. C., Sampaio, C. H., Saucier, C., & Dias, S. L. P. (2016). Activated carbon from sewage sludge for removal of sodium diclofenac and nimesulide from aqueous solutions. *Korean Journal of Chemical Engineering, 33*(11), 3149–3161.

Hadi, P., Xu, M., Ning, C., Lin, C. S. K., & McKay, G. (2015). A critical review on preparation, characterization and utilization of sludge-derived activated carbons for wastewater treatment. *Chemical Engineering Journal, 260*, 895–906.

Kacan, E. (2016). Optimum BET surface areas for activated carbon produced from textile sewage sludges and its application as dye removal. *Journal of Environmental Management, 166*, 116–123.

Kazak, O., Eker, Y. R., Bingol, H., & Tor, A. (2018). Preparation of chemically-activated high surface area carbon from waste vinasse and its efficiency as adsorbent material. *Journal of Molecular Liquids, 272*, 189–197.

Kimura, K., Honoki, D., & Sato, T. (2017). Effective physical cleaning and adequate membrane flux for direct membrane filtration (DMF) of municipal wastewater: up-concentration of organic matter for efficient energy recovery. *Separation and Purification Technology, 181*, 37–43.

Kuroda, S., Nagaishi, T., Kameyama, M., Koido, K., Seo, Y., & Dowaki, K. (2018). Hydroxyl aluminium silicate clay for biohydrogen purification by pressure swing adsorption: Physical properties, adsorption isotherm, multicomponent breakthrough curve modelling, and cycle simulation. *International Journal of Hydrogen Energy, 43*, 16573–16588.

Ladavos, A. K., Katsoulidis, A. P., Iosifidis, A., Triantafyllidis, K. S., Pinnavaia, T. J., & Pomonis, P. J. (2012). The BET equation, the inflection points of N_2 adsorption isotherms and the estimation of specific surface area of porous solids. *Microporous and Mesoporous Materials, 151*, 126–133.

Lapham, D. P., & Lapham, J. L. (2017). Gas adsorption on commercial magnesium stearate: effects of degassing conditions on nitrogen BET surface area and isotherm characteristics. *International Journal of Pharmaceutics, 530*, 364–376.

Li, W. H., Yue, Q. Y., Gao, B. Y., Ma, Z. H., Li, Y. J., & Zhao, H. X. (2011). Preparation and utilization of sludge-based activated carbon for the adsorption of dyes from aqueous solutions. *Chemical Engineering Journal, 171*, 320–327.

Li, F., Lei, T., Zhang, Y., Wei, J., & Yang, Y. (2015). Preparation, characterization of sludge adsorbent and investigations on its removal of hydrogen sulfide under room temperature. *Frontiers of Environmental Science & Engineering, 9*(2), 190–196.

Li, J., Xing, X., Li, J., Shi, M., Lin, A., Xu, C., Zheng, J., & Li, R. (2018). Preparation of thiol-functionalized activated carbon from sewage sludge with coal blending for heavy metal removal from contaminated water. *Environmental Pollution, 234*, 677–683.

Li, D., Zhou, J., Wang, Y., Tian, Y., Wei, L., Zhang, Z., Qiao, Y., & Li, J. (2019). Effects of activation temperature on densities and volumetric CO2 adsorption performance of alkali-activated carbons. *Fuel, 238*, 232–239.

Li, Y. H., Chang, F. M., Huang, B., Song, Y. P., Zhao, H. Y., & Wang, K. J. (2020). Activated carbon preparation from pyrolysis char of sewage sludge and its adsorption performance for organic compounds in sewage. *Fuel, 266*, 117053.

Mininni, G., Blanch, A. R., Lucena, F., & Berselli, S. (2015). EU policy on sewage sludge utilization and perspectives on new approaches of sludge management. *Environmental Science and Pollution Research, 22*, 7361–7374.

Pandiarajan, A., Kamaraj, R., Vasudevan, S., & Vasudevan, S. (2018). OPAC (orange peel activated carbon) derived from waste orange peel for the adsorption of chlorophenoxyacetic acid herbicides from water: adsorption isotherm, kinetic

modelling and thermodynamic studies. *Bioresource Technology, 261*, 329–341.

Peng, L., Dai, H., Wu, Y., Peng, Y., & Lu, X. (2018). A comprehensive review of the available media and approaches for phosphorus recovery from wastewater. *Water, Air, and Soil Pollution, 229*.

Pezoti, O., Cazetta, A. L., Bedin, K. C., Souza, L. S., Martins, A. C., Silva, T. L., Santos Júnior, O. O., Visentainer, J. V., & Almeida, V. C. (2016). NaOH-activated carbon of high surface area produced from guava seeds as a high-efficiency adsorbent for amoxicillin removal: kinetic, isotherm and thermodynamic studies. *Chemical Engineering Journal, 288*, 778–788.

Ping, Q., Zheng, M., Dai, X., & Li, Y. (2020). Metagenomic characterization of the enhanced performance of anaerobic fermentation of waste activated sludge with CaO_2 addition at ambient temperature: fatty acid biosynthesis metabolic pathway and CAZymes. *Water Research, 170*, 115309.

Qiu, M., & Huang, C. (2015). Removal of dyes from aqueous solution by activated carbon from sewage sludge of the municipal wastewater treatment plant. *Desalination and Water Treatment, 53*, 3641–3648.

Rawal, S., Joshi, B., & Kumar, Y. (2018). Synthesis and characterization of activated carbon from the biomass of Saccharum bengalense for electrochemical supercapacitors. *The Journal of Energy Storage, 20*, 418–426.

Satya Sai, P. M., & Krishnaiah, K. (2005). Development of the pore-size distribution in activated carbon produced from coconut shell char in a fluidized-bed reactor. *Industrial and Engineering Chemistry Research, 44*, 51–60.

Shen, F., Liu, J., Zhang, Z., Dong, Y., & Gu, C. (2018). Density functional study of hydrogen sulfide adsorption mechanism on activated carbon. *Fuel Processing Technology, 171*, 258–264.

Sing, K. S. W., Everett, D. H., Haul, R. A. W., Moscou, L., Pierotti, R. A., Rouquerol, J., & Siemieniewska, T. (1985). Reporting physisorption data for gas/solid systems with special reference to the determination of surface area and porosity. *Pure and Applied Chemistry, 57*.

Sulaiman, N. S., Hashim, R., Mohamad Amini, M. H., Danish, M., & Sulaiman, O. (2018). Optimization of activated carbon preparation from cassava stem using response surface methodology on surface area and yield. *Journal of Cleaner Production, 198*, 1422–1430.

Sun, K., Huang, Q., Chi, Y., & Yan, J. (2018). Effect of ZnCl2-activated biochar on catalytic pyrolysis of mixed waste plastics for producing aromatic-enriched oil. *Waste Management, 81*, 128–137.

Tian, D., Xu, Z., Zhang, D., Chen, W., Cai, J., Deng, H., Sun, Z., & Zhou, Y. (2019). Micro–mesoporous carbon from cotton waste activated by FeCl3/ZnCl2: preparation, optimization, characterization and adsorption of methylene blue and eriochrome black T. *Journal of Solid State Chemistry, 269*, 580–587.

Wang, X., Zhu, N., & Yin, B. (2008). Preparation of sludge-based activated carbon and its application in dye wastewater treatment. *Journal of Hazardous Materials, 153*, 22–27.

Wang, N., Zhang, W., Cao, B., Yang, P., Cui, F., & Wang, D. (2018). Advanced anaerobic digested sludge dewaterability enhancement using sludge based activated carbon (SBAC) in combination with organic polymers. *Chemical Engineering Journal, 350*, 660–672.

Wei Yu, K. S. (2018). Modeling gas adsorption in Marcellus shale using Langmuir and BET isotherms. In *Shale gas and tight oil reservoir simulation* (pp. 129–154).

Ye, Y., Ngo, H. H., Guo, W., Liu, Y., Chang, S. W., Nguyen, D. D., Liang, H., & Wang, J. (2018). A critical review on ammonium recovery from wastewater for sustainable wastewater management. *Bioresource Technology, 268*, 749–758.

Zhang, J. P., Sun, Y., Woo, M. W., Zhang, L., & Xu, K. Z. (2016). Preparation of steam activated carbon from black liquor by flue gas precipitation and its performance in hydrogen sulfide removal: experimental and simulation works. *Revista Mexicana de Urología, 76*, 395–404.

Zhang, Y., Song, X., Xu, Y., Shen, H., & Kong, X. (2019). Utilization of wheat bran for producing activated carbon with high speci fi c surface area via NaOH activation using industrial furnace. *Journal of Cleaner Production, 210*, 366–375.

Zhu, J., Li, Y. H., Xu, L., & Liu, Z. Y. (2018). Removal of toluene from waste gas by adsorption-desorption process using corncob-based activated carbons as adsorbents. *Ecotoxicology and Environmental Safety, 165*, 115–125.

Publisher's Note Springer Nature remains neutral with regard to jurisdictional claims in published maps and institutional affiliations.